ISCI, Volume *13*

Supplemental Information

The RNA Processing Factor Y14 Participates in DNA Damage Response and Repair

Tzu-Wei Chuang, Chia-Chen Lu, Chun-Hao Su, Pei-Yu Wu, Sarasvathi Easwvaran, Chi-Chieh Lee, Hung-Che Kuo, Kuan-Yang Hung, Kuo-Ming Lee, Ching-Yen Tsai, and Woan-Yuh Tarn

Supplemental Information (SI)

Supplemental Tables

Table S1: Mass-spectrometric Analysis of Y14-interacting Proteins. (Related to Table 1).

FLAG-Y14 was immunoprecipitated from HEK293 cells using anti-FLAG; co-immunoprecipitates identified by mass spectrometric analysis are functionally categorized.

Table S2: Primers Used in This Study. (Related to Figures 6 and S5).

Experiments/ Gene names	Sequences (5' to 3')
DRIP	
Egr1-F	TTCGGATTCCCGCAGTGT
Egr1-R	TCACTTTCCCCCCTTTATCCA
Apoe-F	CCGGTGAGAAGCGCAGTCGG
Apoe-R	CCCAAGCCCGACCCCGAGTA
Rpl13A-F	GCTTCCAGCACAGGACAGGTAT
Rpl13A-R	CACCCACTACCCGAGTTCAAG
Btbd19-F	CCCCAAAGGGTGGTGACTT
Btbd19-R	TTCACATTACCCAGACCAGACTGT
Intergenic-F	CTGTACCTGGGGTTCATTCATT
Intergenic-R	CAGTAAGCCGTTCACTCTCAC
End-joining assay	
GFP-F	GCTGGACGGCGACGTAAAC
GFP-R	GGTCTTGTAGTTGCCGTC
ChIP	
DR-GFP-F	CATGCCCGAAGGCTACGT
DR-GFP-R	CGGCGCGGGTCTTGTA

F, forward; R, reverse; TSS, transcription start site; GB, gene body

Figure S1

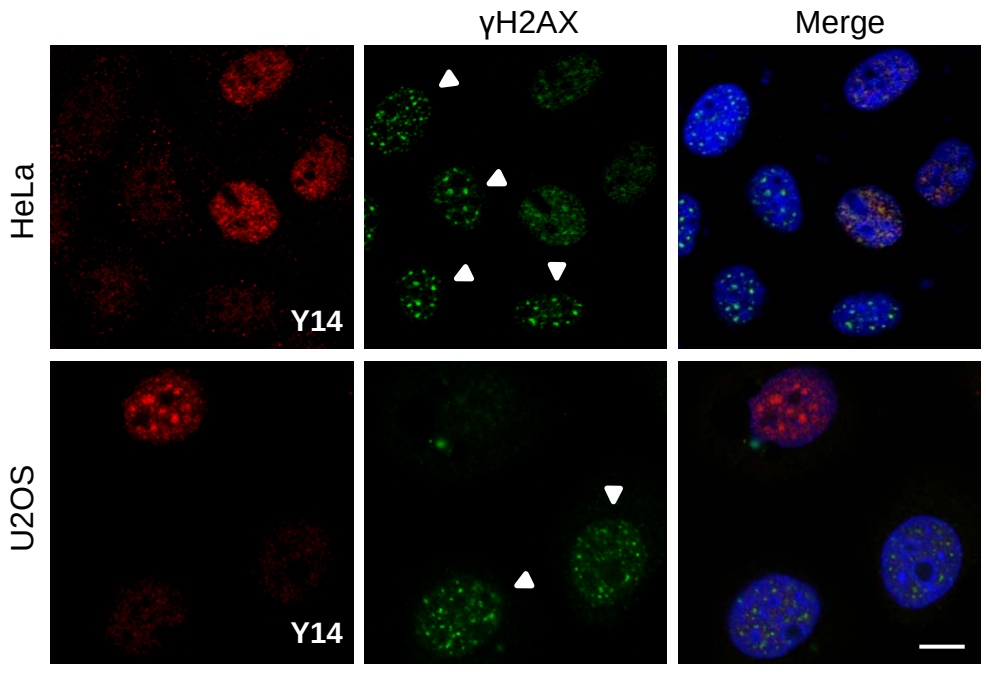

Figure S2

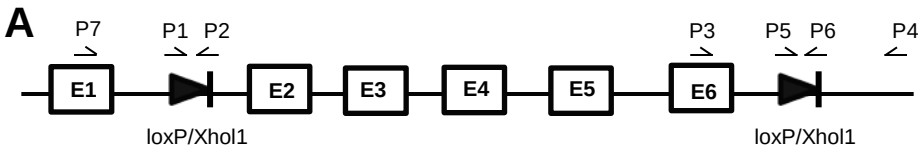
A
P7
P1 P2
P3
P5 P6
P4
E1
E2
E3
E4
E5
E6
loxP/Xhol1
loxP/Xhol1

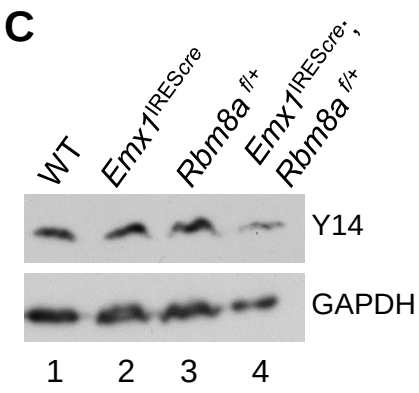
C
WT
Emx1IREScre
Rbm8a f/+
Emx1IREScre; Rbm8a f/+
Y14
GAPDH
1 2 3 4

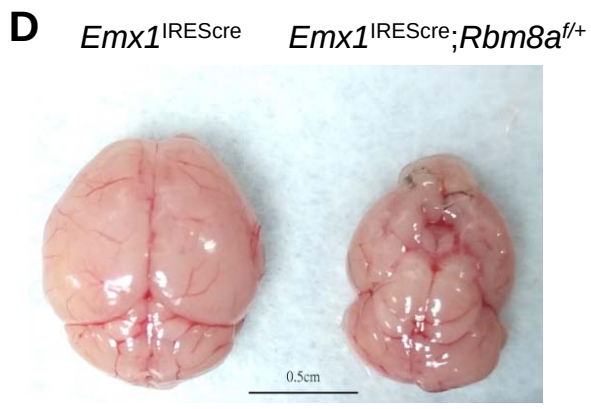
D
Emx1IREScre
Emx1IREScre;Rbm8af/+
0.5cm

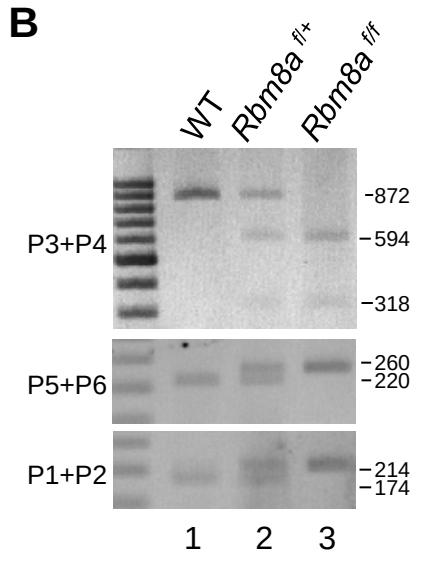
B
WT
Rbm8a f/+
Rbm8a f/f
P3+P4
P5+P6
P1+P2
872
594
318
260
220
214
174
1 2 3

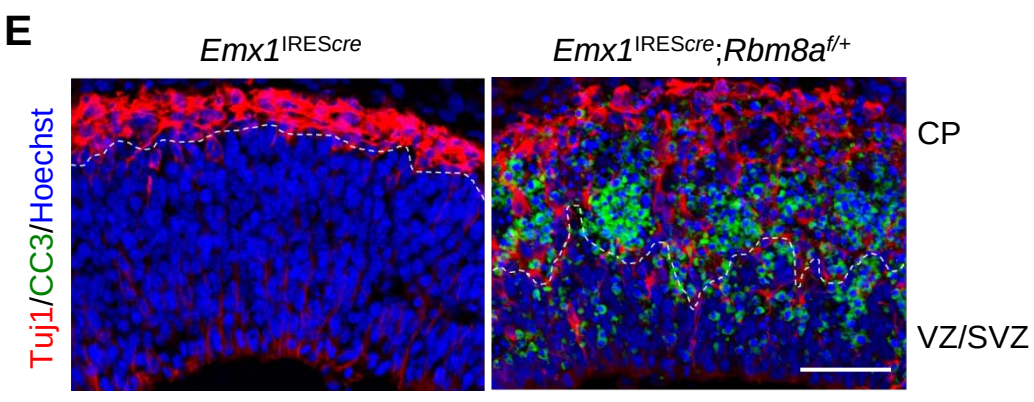
E
Emx1IREScre
Emx1IREScre;Rbm8af/+
Tuj1/CC3/Hoechst
CP
VZ/SVZ

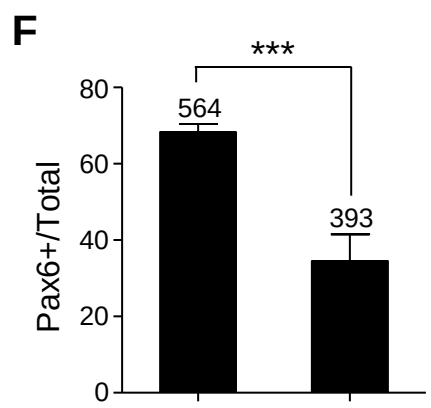
F
***
Pax6+/Total
80
60
40
20
0
564
393

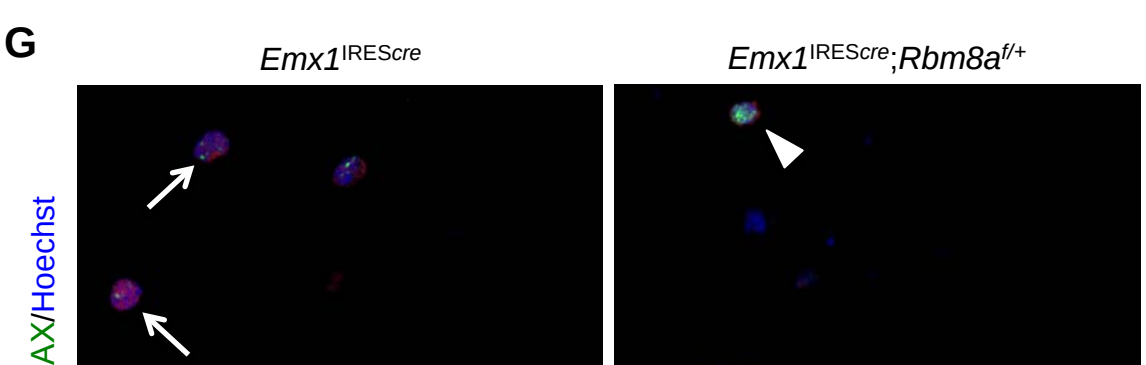
G
Emx1IREScre
Emx1IREScre;Rbm8af/+
Pax6/γH2AX/Hoechst
Pax6/CC3/Hoechst

Figure S3

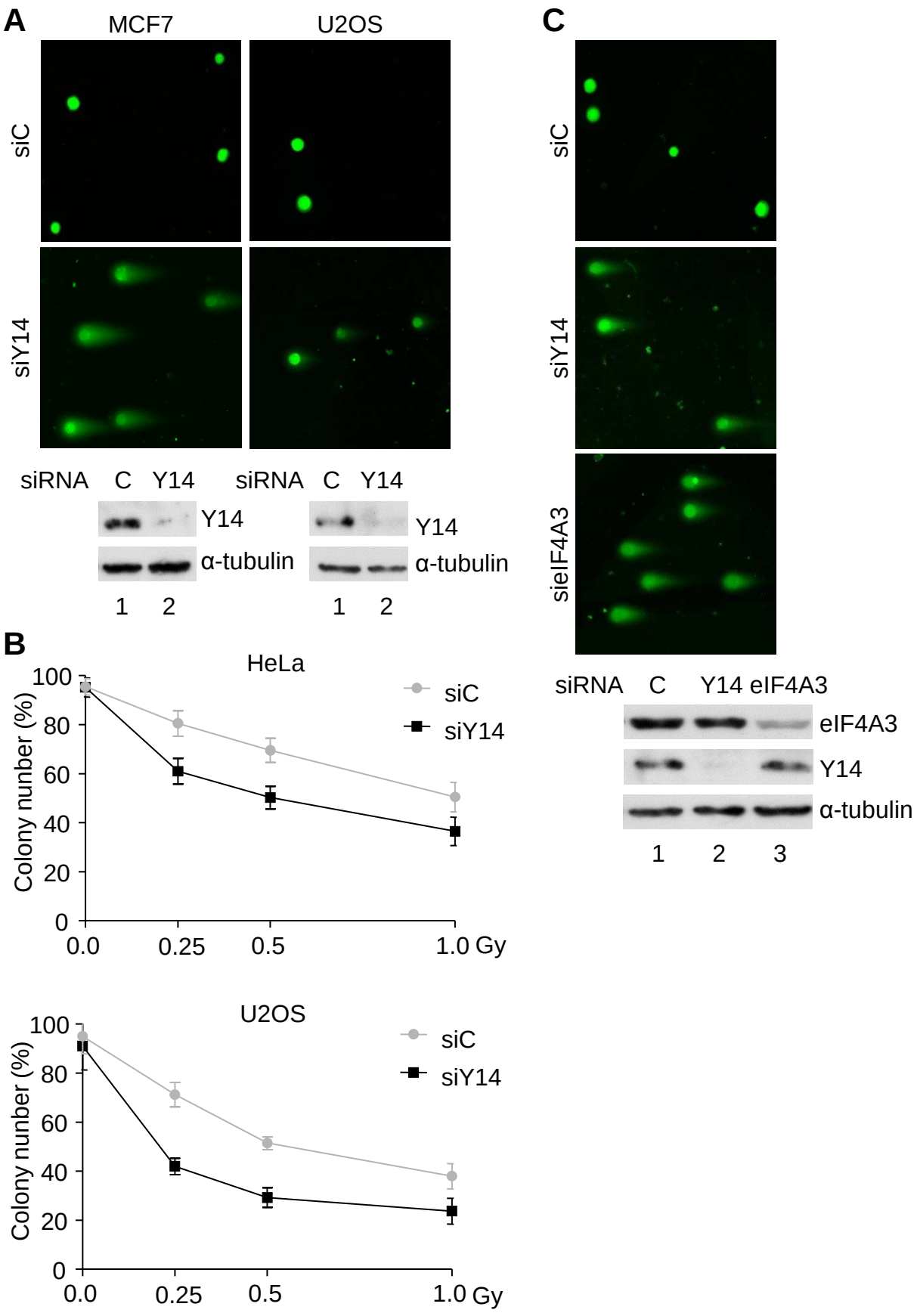
A
MCF7
U2OS
siC
siY14
siRNA C Y14
Y14
α-tubulin
1 2
B
HeLa
siC
siY14
Colony nunber (%)
0 20 40 60 80 100
0.0 0.25 0.5 1.0 Gy
U2OS
C
siC
siY14
sieIF4A3
siRNA C Y14 eIF4A3
eIF4A3
Y14
α-tubulin
1 2 3

Figure S4

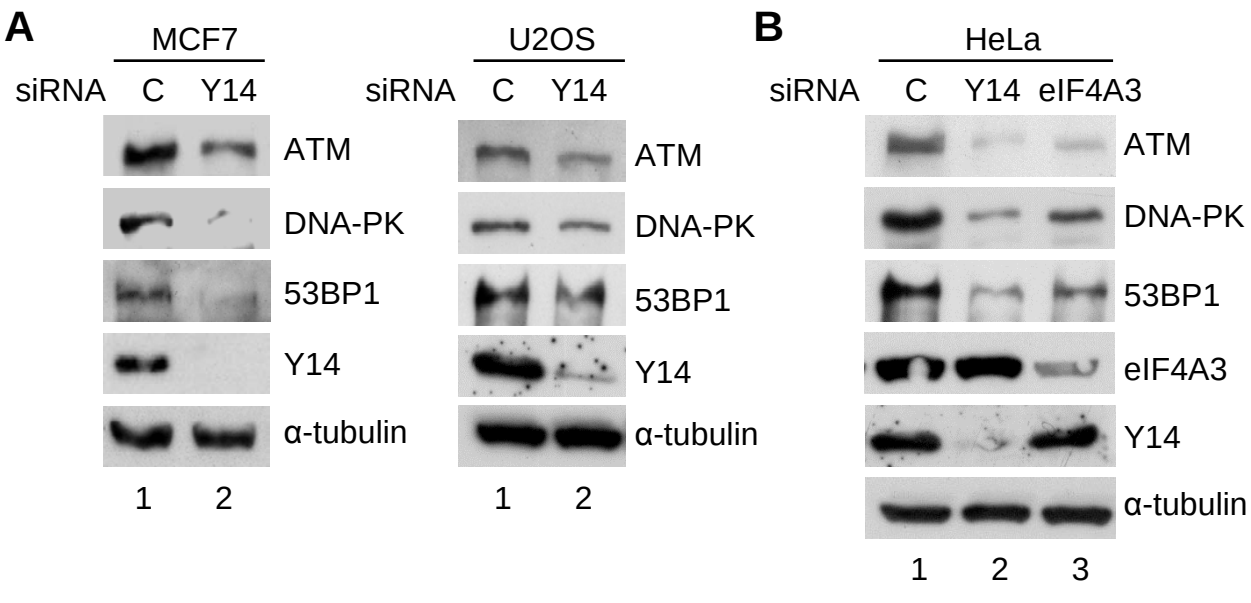
A
MCF7
siRNA C Y14
ATM
DNA-PK
53BP1
Y14
α-tubulin
1 2
U2OS
siRNA C Y14
ATM
DNA-PK
53BP1
Y14
α-tubulin
1 2
B
HeLa
siRNA C Y14 eIF4A3
ATM
DNA-PK
53BP1
eIF4A3
Y14
α-tubulin
1 2 3

Figure S5

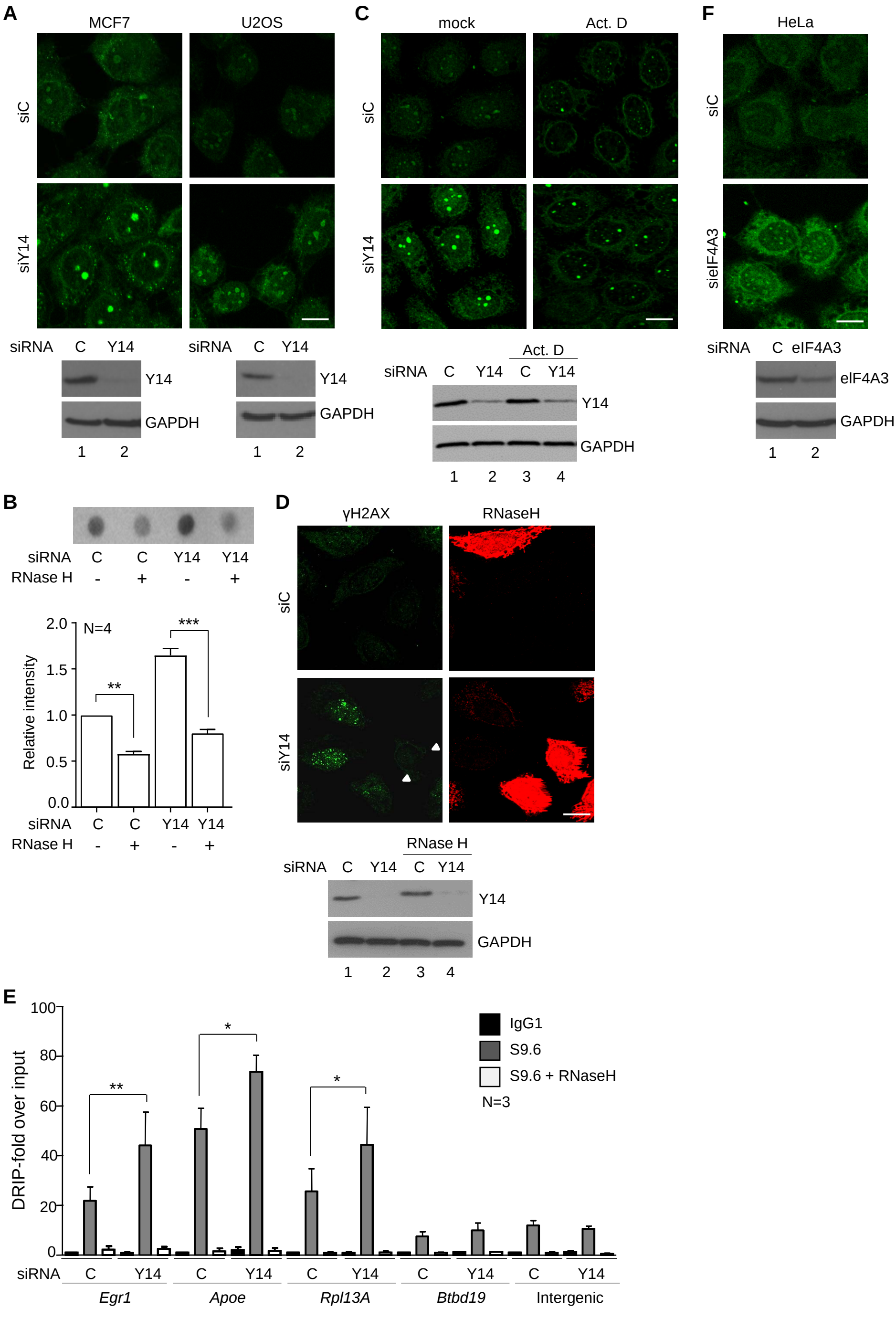
A
MCF7
U2OS
siC
siY14
siRNA C Y14
Y14
GAPDH
1 2
C
mock
Act. D
Act. D
siRNA C Y14 C Y14
F
HeLa
sieIF4A3
siRNA C eIF4A3
eIF4A3
B
siRNA C C Y14 Y14
RNase H - + - +
N=4
Relative intensity
2.0
1.5
1.0
0.5
0.0
**
***
D
γH2AX
RNaseH
RNase H
1 2 3 4
E
DRIP-fold over input
100
80
60
40
20
0
*
IgG1
S9.6
S9.6 + RNaseH
N=3
Egr1
Apoe
Rpl13A
Btbd19
Intergenic

Figure S6

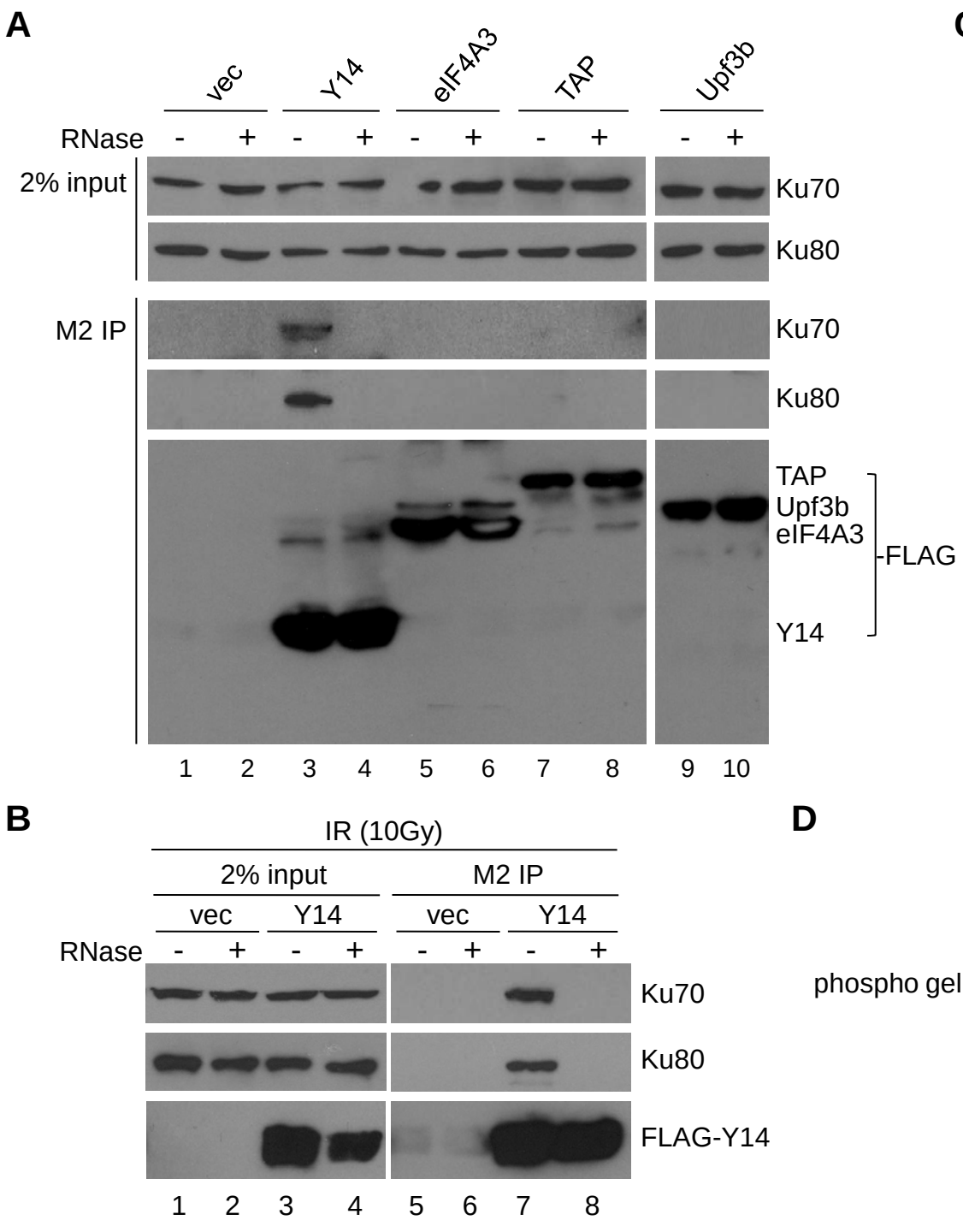
A
vec
Y14
eIF4A3
TAP
Upf3b
RNase
- + - + - + - + - +
2% input
Ku70
Ku80
M2 IP
Ku70
Ku80
TAP
Upf3b
eIF4A3
Y14
FLAG
1 2 3 4 5 6 7 8 9 10
B
IR (10Gy)
2% input
M2 IP
vec
Y14
vec
Y14
RNase
- + - + - + - +
Ku70
Ku80
FLAG-Y14
1 2 3 4 5 6 7 8
C
2% input
M2 IP
siATM
- + - +
vec
Y14
vec
Y14
vec
Y14
vec
Y14
ATM
Ku70
Ku80
Trim28
γH2AX
H2AX
FLAG-Y14
1 2 3 4 5 6 7 8
D
vec
FLAG-Y14
-
Caffeine
KU55933
-
Caffeine
KU55933
phospho gel
**
**
*
1 2 3 4 5 6

Figure S7

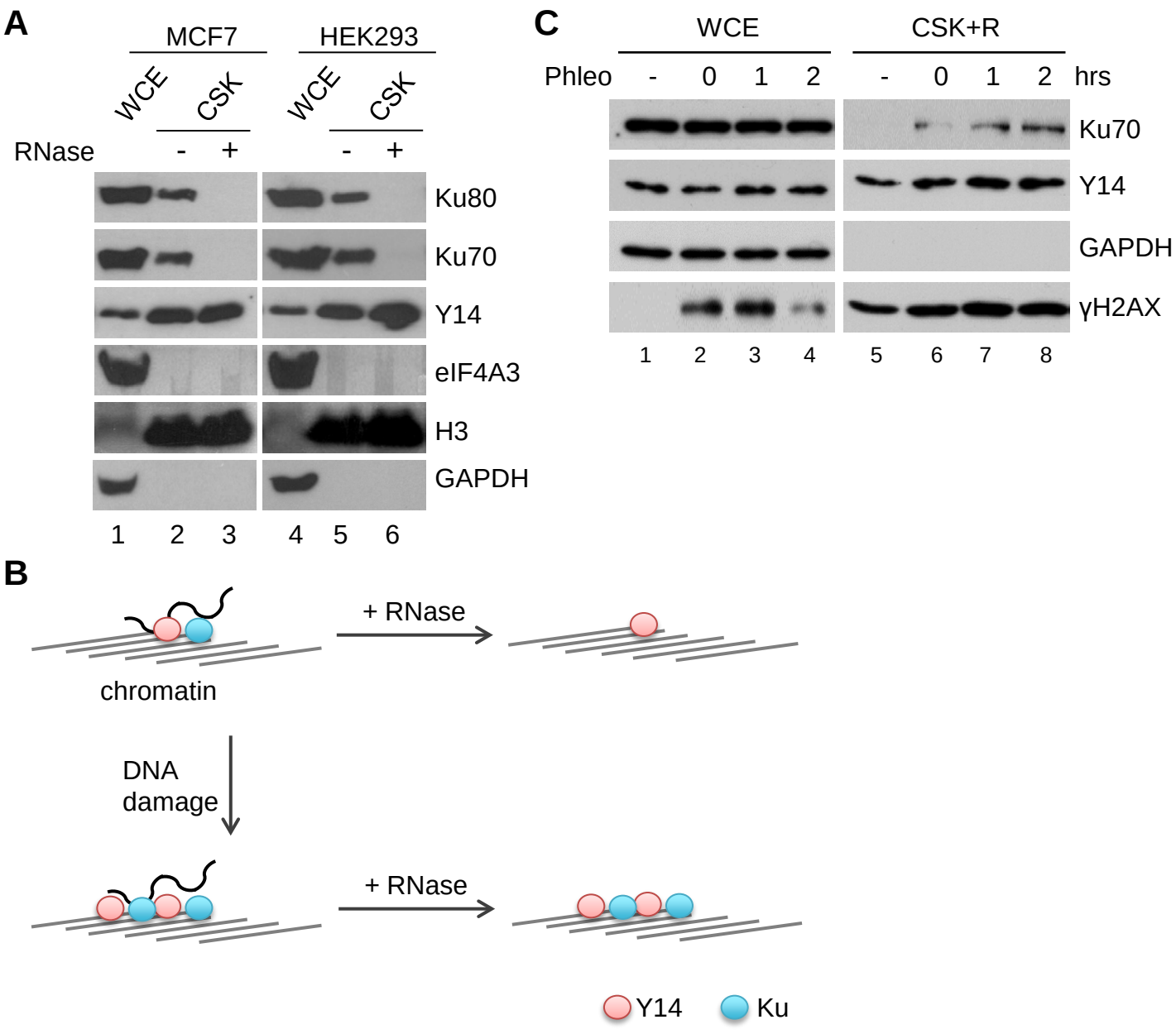
A
MCF7
HEK293
WCE
CSK
WCE
CSK
RNase
- +
- +
Ku80
Ku70
Y14
eIF4A3
H3
GAPDH
1 2 3 4 5 6
C
WCE
CSK+R
Phleo - 0 1 2 - 0 1 2 hrs
Ku70
Y14
GAPDH
γH2AX
1 2 3 4 5 6 7 8
B
+ RNase
chromatin
DNA
damage
+ RNase
Y14
Ku

Figure S8

WCE
CSK+R
siC
sieIF4A3
Post-Phleo
- 0 2 - 0 2
- 0 2 - 0 2
Ku70
Ku80
eIF4A3
GAPDH
H3
1 2 3 4 5 6 7 8 9 10 11 12
Chromatin-bound Ku70
Chromatin-bound Ku80
2.0
1.5
1.0
0.5
0.0
siC
sieIF4A3
- 0 2 hrs
Post-Phleo

Figure S9

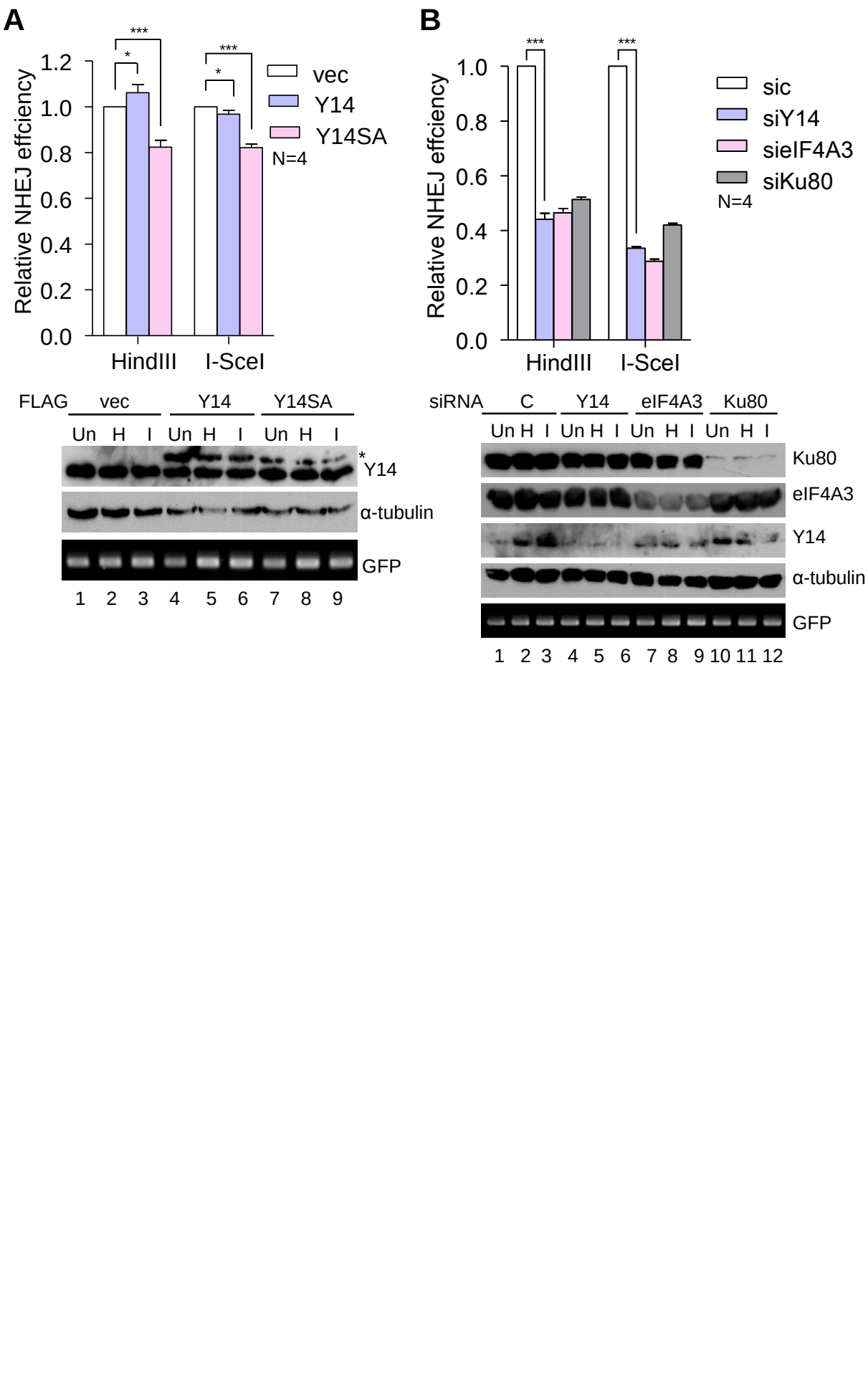
A
B
Relative NHEJ effciency
vec
Y14
Y14SA
N=4
HindIII
I-SceI
sic
siY14
sieIF4A3
siKu80
FLAG
siRNA
C
eIF4A3
Ku80
Un H I
Y14
α-tubulin
GFP
1 2 3 4 5 6 7 8 9
1 2 3 4 5 6 7 8 9 10 11 12

Supplemental Figure Legends

Figure S1. Y14 Depletion Induced γH2AX Foci. (Related to Figure 1).

HeLa and U2OS cells were transfected with siC or siY14 and subjected to immunostaining using anti-γH2AX and anti-Y14 and Hoechst staining. Arrowhead indicates Y14-depleted cells. Scale bar, 10 μm.

Figure S2. Generation and Characterization of the *Emx1*^{IREScre}*;Rbm8a*$^{f/+}$ Embryonic Brain. (Related to Figure 1).

(A) Schematic diagram shows the engineered mouse *Rbm8a* gene, in which the two loxp sites (arrowheads) were inserted into intron 1 and the 3' end, respectively. Primers used for genotyping are depicted; their sequences are listed in Table S2.

(B) Genotyping of *Rbm8a* floxed mice. PCR using P3 and P4 generated a 872-bp band. After *Xho*I digestion, the loxp-containing product generated two bands of 594 bp and 318 bp, respectively. PCR using P5 and P6 generated a 220-bp band in the wild-type and a 260-bp band in the loxp-containing allele. PCR using P1 and P2 generated a 174-bp band in the wild-type and a 214-bp band in the loxp-containing allele.

(C) Immunoblotting shows Y14 and GAPDH proteins in E13.5 dorsal neocortex lysates with indicated genotypes.

(D) The brain of *Emx1*^{IREScre} and *Emx1*^{IREScre}*;Rbm8a*$^{f/+}$ at postnatal day 10.

(E) Immunofluorescence of E13.5 dorsal neocortices of *Emx1*^{IREScre} and *Emx1*^{IREScre}*;Rbm8a*$^{f/+}$ using antibodies against activated caspase 3 (CC3, green) and Tuj1 (red) and Hoechst staining (blue) were performed. CP, cortical plate; VZ, ventricular zone; SVZ, subventricular zone. Scale bar, 50 μm.

(F) Bar graph shows percentage of Pax6+ cells/total cells that were observed by immunostaining using anti-Pax6 and Hoechst staining as in panel G. The number of the cells (from three pairs of littermates) analyzed is indicated.

(G) Immunostaining and Hoechst staining of primary cells dissociated from the dorsal neocortices of *Emx1*^{IREScre} and *Emx1*^{IREScre}*;Rbm8a*$^{f/+}$ embryos. Upper and lower representative images show immunostaining of Pax6/γH2AX and Pax6/CC3, respectively; all were merged with Hoechst staining. Arrows and arrowheads depict Pax6-expressing cells without or with γH2AX (upper) or CC3 (lower), respectively. Scale bar, 25 μm.

Figure S3. Depletion of Y14 Causes DNA Damage and Sensitizes Cells to IR-induced Apoptosis. (Related to Figure 2).

(A) The neutral comet assay was performed in Y14-depleted MCF7 and U2OS cells. The comet tail was barely detected in the latter.

(B) siC or siY14-transfected HeLa and U2OS cells were exposed to increasing doses of IR followed by Clonogenic assay as in Figure 2B. Curve graphs show relative percentage of cell survival after different doses of IR. For each transfectant, the number of survived cells after IR was normalized to that of mock-treated cells. Mean ± SD were obtained from three independent experiments.

(C) The neutral comet assay was performed in siC, siY14 or eIF4A3-depleted HeLa cells.

Figure S4. Y14 Depletion Compromises the Expression of DDR Factors in Various Cell Lines. (Related to Figure 2).

(A) Immunoblotting of siC or siY14-transfected MCF7 and U2OS cell lysates was performed using antibodies against indicated proteins.
(B) Immunoblotting of siC, siY14 or sieIF4A3-transfected HeLa cell lysates.

Figure S5. Y14 Depletion-induced Transcription-dependent R-loops. (Related to Figure 2).
(A) Immunofluorescence detection of R-loops using antibody S9.6 in Y14-depleted MCF7 and U2OS cells. Scale bar in all cell images, 10 μm.
(B) Genomic DNA of siRNA-transfected HeLa cells was either left untreated or treated with RNase H and subjected to dot blot analysis using S9.6. Bar graph shows fold changes (mean ± SD) of S9.6 signals (non-RNase H treated siC was set as 1).
(C) siC or siY14-transfected HeLa cells were treated with 4 μM actinomycin D for 4 hrs, followed by immunofluorescence using antibody S9.6.
(D) HeLa cells were co-transfected with siC or siY14 and pcDNA3-RNase H1. Immunofluorescence was performed using anti-γH2AX and anti-RNase H1. siY14/RNase H-expressing cells (arrowhead) exhibited reduced γH2AX signals.
(E) DRIP using S9.6 was performed with siRNA-transfected HeLa cell lysates. Precipitates were mock treated or treated with RNase H, followed by qPCR using gene specific primers. For each DRIP, the precipitation efficiency (IP/input) was measured. Bar graph represents relative fold-enrichment (mean ± SEM) of the DNA-RNA hybrid for each gene (IgG was set as 1). *p*-values: * < 0.01, ** < 0.05, *** <0.001.
(F) Immunofluorescence of eIF4A3-depleted HeLa cells was performed as panel A.

Figure S6. Y14 Associates with Chromatin and its Phosphorylation is Abolished by ATM Inhibition. (Related to Figure 3).
(A) HEK293 cells were transfected with the empty vector or vector encoding FLAG-tagged Y14, eIF4A3, TAP or Upf3b. Immunoprecipitation using anti-FLAG was performed followed by immunoblotting.
(B) HEK293 cells were transfected with the empty or FLAG-Y14 vector, and exposed to 10 Gy IR. The lysates were mock-treated or treated with RNase, followed by immunoprecipitation and immunoblotting.
(C) HEK293 cells were transfected with siC or siATM and the empty or FLAG-Y14 vector. The cell lysates were subjected to immunoprecipitation using anti-FLAG, followed by immunoblotting.
(D) HEK293 cells were transiently transfected with the empty or FLAG-Y14 vector, and then mock-treated or treated with caffeine or KU55933. The cell lysates were analyzed by electrophoresis on a phosphate-affinity gel, followed by immunoblotting using anti-FLAG. **, hyperphosphorylated Y14; *, hypophosphorylated Y14.

Figure S7. Subnuclear Fractionation Reveals Chromatin-Associated Y14 prior to or post-DNA Damage. (Related to Figure 4).
(A) Immunoblotting of the whole cell extract (WCE) and RNase-treated (+) and non-treated (-) chromatin fractions (CSK) of MCF and HEK293 cells.
(B) Diagram shows RNA-mediated association of Y14 and Ku. After RNase treatment, only Y14 remained bound to chromatin. After DNA damage, chromatin localization of both proteins was enhanced and became RNase resistant.

(C) HeLa cells were mock-treated (-) or treated with phleomycin followed by recovery for 0, 1 or 2 hrs. Immunoblotting of the WCE and CSK+R fraction was performed using antibodies against indicated proteins.

Figure S8. Depletion of eIF4A3 Does Not Significantly Enhance Ku Retention on Chromatin. (Related to Figure 4).
HeLa cells were transfected with sieIF4A3, followed by phleomycin treatment, chromatin fractionation, and immunoblotting, as in Figure 6A. Bar graph shows the relative level of chromatin-bound Ku70 (left) and Ku80 (right) in siC and sieIF4A3 cells (lane 7 was set as 1).

Figure S9. Y14 Depletion Impairs DNA Repair in HeLa Cells. (Related to Figure 6).
(A) The end-joining assay was performed in HeLa cells. The uncut or cut (*Hind*III or I-*Sce*I) NHEJ reporter was co-transfected with siRNA (control, Y14, eIF4A3 or Ku80) into HeLa cells. Bar graphs show relative end-joining efficiency. Immunoblotting and PCR of GFP were performed as in Figure 6C-E. Asterisk indicates FLAG-Y14. *p*-values: * < 0.01, *** <0.001.
(B) The assay was performed as in panel A, except that cells were transfected with the indicated expression vector (empty, FLAG-Y14 or FLAG-Y14SA). *p*-values: * < 0.01, *** <0.001.

Transparent Methods

Cell Culture, Transfection and Drug Treatment

Culture and transient transfection of HeLa, HEK293, MCF7 and U2OS cells were carried out essentially as described (Chuang et al., 2013). U2OS stable cells containing a homology-directed repair (HDR) reporter (DR-GFP) were a kind gift of J. M. Stark and cultured as described (Gunn et al., 2011). Cells were, in general, collected 48 h after transfection with a siRNA or expression vector. Three siRNAs used including siY14, sieIF4A3 and negative control LO GC (Invitrogen) were previously describe (Lu et al., 2017). For DNA damage induction, cells were irradiated with various doses of X-rays or treated with 500 μM phleomycin (InvivoGen). For pharmacological treatment, cells were treated with actinomycin D (4 μM, Sigma-Aldrich) for 4 hrs, ATM inhibitor KU55933 (10 μM; Tocris) for 1 h prior to IR, caffeine (2 mM; Sigma) for 24 h or 5,6-dichloro-1-β-D-ribofuranosylbenzimidazole (DRB) (100 μM; Sigma) for 3 h prior cell harvest.

Plasmids and siRNAs

The expression vectors encoding FLAG-tagged Y14, Y14-SA and eIF4A3 and HA-tagged ubiquitin were previously described (Hsu Ia et al., 2005; Chuang et al., 2013; Lu et al., 2017). The pLKO.1-shY14-mCherry vector was constructed by replacing the puromycin sequence of pLKO.1-shY14 (Academia Sinica RNAi Core, Taipei) with mCherry; the shY14 sequence was CCGGCGAGAGCATTCACAAACTGAACTCGAGTTCAGTTTGTGAATGCTCTCGTTTTTG). The NHEJ reporter GFP-Pem1-Ad2 was a kind gift of Vera Gorbunova (University of Rochester (Seluanov et al., 2004). The I-*Sce*I expression vector pCB-ASce was obtained from Jeremy M. Stark (Beckman Research Institute of City of Hope, Duarte; (Gunn et al., 2011). The pEGFP-C1-FLAG-Ku70 was purchased from Addgene. The pcDNA3-RNase H1 was a kind gift from Andres Anguilera (Universidad de Sevilla, Servilla)(Bhatia et al., 2014). The GST-TAP and GST-Upf3b expression vectors were described (Chuang et al., 2011). siRNA targeting ATM was 5'-AGUCUAGUACUUAAUGAUCUGCUUA-3' (Invitrogen).

Conditional Knockout of *Rbm8a* in Mice

The two *loxp* sequences were inserted into intron 1 and the 3' end of *Rbm8a* using CRISPR/Cas9 to generate *Rbm8a* conditional allele. The guide RNA sequences used are 5'-GATAGTCTAGGAAACGCGAC and 5'- CCACCACTACACAGTGGTTT, respectively. The 5' (5'-gaagcaacaaaaataagagtcatttgaaaaaaaaaacaaaaaaaacctgtcCTCGAGATAACTTCGTATAATGTATGCTATACGAAGTTATgcgtttcctagactatctggaagcttcgacacagactccagcttcagtcccttcccagttccgccctaattcctttcccaaggggggaggagtctatcttttcagaccc) and 3' (5'-gatagtatataaacatacatgcaggcaaaaacctcattagatatttaaaccaaaaCTCGAGATAACTTCGTATAATGTATGCTATACGAAGTTATccactgtgtagtggtggtgcatgcctttgataccagccttgggaggaagaggcaggtagatctttctttgtgagttccagaccagcctggagaaagaaagtgggg) single strand HDR templates containing the *loxp* sequence (upper class) and *Xho*I (upper class and underlined) site were synthesized by IDT (Integrated DNA Technologies). The T7 promoter sequence (5'-TTAATACGACTCACTATA) was added upstream of gRNA sequence and a partial tracrRNA sequence (5'- GTTTTAGAGCTAGAAATAGC) was added downstream of the gRNA sequence. The oligonucleotide was annealed with reverse tracrRNA (5'-

TTTAAAAGCACCGACTCGGTGCCACTTTTTCAAGTTGATAACGGACTAGCCTTATT TTAACTTGCTATTTCTAGCTCTAAAAC) and PCR amplified using Phusion DNA polymerase (Thermo-Fisher Scientific) according to the manufacture's instruction. The amplified product was purified using QIAquick PCR purification Kit (Qiagen) and served as *in vitro* transcription template. The sgRNA were synthesized using HiScribe™ T7 Quick High Yield RNA Synthesis Kit from NEB (NEB). Cas9 mRNA was synthesized using mMESSAGE mMACHINE T7 ULTRA Kit (Thermo-Fisher Scientific), purified using MEGAclear Transcription Clean-up kit (Thermo-Fisher Scientific) and eluted with the injection buffer containing 10 mM Tris-HCl (pH7.2) and 0.1mM EDTA. The quality and quantity of RNAs were analyzed using NanoDrop ND-1000 (Thermo-Fisher Scientific).

For mice production, the 5' *loxp* and 3' *loxp* were inserted by sequential injection of the 5'- and 3'-sgRNA along with Cas9 mRNA and single strand oligonucleotide (ssODN) independently. The 3'-*loxp*-*Xho*I HDR template was first inserted to generate 3'-*loxp* inserted mice. These mice were then used as breeder, and their zygotes were subjected to subsequent injection of 5'-*loxp*. For the injection, Cas9 mRNA, sgRNAs and ssODN were diluted with injection buffer to final concentration of 50, 50 and 100 ng/μl, respectively. Super-ovulated C57BL/6J female mice of 3-4 week old were set mating to male mice and one-cell stage zygotes were collected on the next day. The mixture of Cas9 mRNA, sgRNA and ssODN was injected into both pronuclei and cytoplasm of the zygotes. Injected zygotes were cultured in EmbryoMax KSOM Medium in humidified incubator (37^{o}C, 5% CO_2) for overnight. Two-cell stage embryos were transferred into the oviduct of 0.5-dpc pseudo-pregnant ICR female mice (BioLASCO, Taiwan).

To confirm the 3'-*loxp* knock-in, the 3' end region was PCR amplified using the following primer pair: P3 (5'- CCTCTTCCAGAGGTCCTAAGTCCAA) and P4 (5'- GTAGCAGCAATAGCCTGACTATAGTTGT). For 5'- and 3'-*loxp* knock-in, PCR primers P7 (5'- GAAGATTTCGCCATGGATGAGGATGG) and P4 were used to amplify the region comprising 5'- and 3'-loxp. The PCR product that can be digested with *Hind*III was further sequenced to confirm the two *loxp* sites that remained intact. After genotype confirmation, heterozygous mice (*Rbm8a*$^{f/+}$) were mated to *Emx1*^{IREScre} mice (Gorski et al., 2002) generously provided by Kevin R. Jones (University of Colorado, Boulder) to obtain *Emx1*^{IREScre};*Rbm8a*$^{f/+}$. The *Emx1*^{IREScre} littermates were used as control. The following were also used for genotyping: P1 (5'- CCTTGGGAAAGGAATTAGGGGC), P2 (5'- GTTTGTGGATGCTTTCTAGAGTTCCAG), P5 (5'- GATCTACCTGCCTCT TCCTCCCA) and P6 (5'- GACAGATTGAATCCCCCATCCACA).

All experimental procedures involving animals were approved by the Institutional Animal Care and Use Committee (IUCUC) 17-08-1104 of Academia Sinica and complied with the Ministry of Science and Technology, Taiwan.

Immunostaining and Isolation of Embryonic Brain Cells

The procedure for immunostaining of E13.5 mouse embryonic cortex is described in Supplemental Information. For immunostaining, polyclonal antibodies against γH2AX (Novus), Pax6 (BioLegend) and CC3 (Cell Signaling) and monoclonal antibodies against Y14 (Abcam), Pax6 (DSHB) and Tuj1 (Biolegend) were used. Secondary antibodies used were conjugated with Alexa Fluor 488 (green) or Alexa Fluor 568 (red). To collect primary brain cells, E13.5 embryonic dorsal cortices were dissected and dissociated according to (Mao et al., 2015). Isolated cells were plated on poly-D-lysine-coated coverslips in 6-well

culture dishes and incubated in DMEM-F12 medium supplemented with N2, Glutamax, Non-Essential Amino Acids (NEAA), bFGF, EGF, penicillin-streptomycin, and amphotericin (all from Gibco) at 37°C for 3 h. Attached cells were fixed with 4% paraformaldehyde for 10 min for indirect immunofluorescence and staining with Hoechst.

Neurosphere Formation
Primary brain cells were isolated and incubated in the same medium described as above. Dissociated cells were cultured in Ultra-Low attachment surface plate (Corning) for 10 days. Neurosphere area was measured by Image J.

Colony Formation Assay
siRNA-transfected cells were cultured for 3 weeks and colonies were fixed and stained as described in (Lai et al., 2010).

Neutral Comet Assay
The procedure is described in (Nowsheen et al., 2012). Briefly, after harvest, cells were suspended in 1% low-melting agarose (Sigma) at 10^5 cells/ml and embedded on slides, followed by treatment with cold lysis buffer (2.5 M NaCl, 100 mM EDTA, 10 mM Tris base, 1% sodium lauryl sarcosinate, 1% TritonX-100, pH 10). The slides were subjected to electrophoresis using 1 V/cm for 15 min at 4˚C. After electrophoresis, slides were fixed with ethanol and stained with SYBR green. Images were acquired by using Zeiss confocal 700 microscope, and the tail moment was analyzed using CASP software (CaspLab).

Chromatin Fractionation
The procedure for chromatin fractionation is described in (Britton et al., 2013). Essentially, cells were washed twice with phosphate-buffered saline and then incubated at 4˚C for 3 min in the cytoskeleton (CSK) buffer containing 10 mM PIPES (pH 7.0), 100 mM NaCl, 300 mM sucrose, 3 mM $MgCl_2$, and 0.7% Triton X-100 and optionally supplemented with 0.3 mg/ml RNase A. After centrifugation at 5000×*g* for 3 min, the chromatin-enriched pellet was washed three times with phosphate-buffered saline containing protease inhibitors, and collected in the SDS lysis buffer.

Immunoprecipitation and Mass Spectrometry
The procedure for immunoprecipitation-mass spectrometry was carried out essentially as previously described (Lee and Tarn, 2014). In brief, approximately 1.5×10^7 HEK293 cells were transiently transfected with 20 μg of pCDNA-FLAG-Y14. The cell lysate was prepared and subjected to immunoprecipitation using anti-FLAG M2 affinity gel (Sigma). For mass spectrometry, immunoprecipitates were fractionated on SDS-polyacrylamide gels and stained with SYPRO-Ruby (Bio-Rad). The bands of interest were excised, trypsinized and subjected to liquid chromatography coupled with tandem mass spectrometry (LTQ XL, ThermoFinnigan). For the analysis of mass spectrometry data, the Voyager-DE STR Biospectrometry Workstation (Applied Biosystems) and Mascot software (www.matrixscience.com) were used. Polyclonal anti-Y14 (Bethyl) and anti-Ku80 (Cell Signaling Technology) were used for immunoprecipitation of endogenous Y14 and Ku. Rabbit IgG (Bethyl) was used as control.

Immunoblotting
Immunoblotting was performed according to Chuang et al. (2013). Monoclonal antibodies used were against RNA pol II C-terminal domain (CTD) (Abcam), ATM, Mre11, and Nbs1 (Genetex), Chk1 (Santa Cruz Biotechnology), Chk2 (MBL), GAPDH (ProteinTech) and α-tubulin (NeoMarkers). Polyclonal antibodies used were against FLAG epitope (Sigma), HA epitope (Bioman), Y14, MDC1, XLF, Trim28 (Bethyl), γH2AX, 53BP1 (Novus), DNA ligase IV (Acris), XRCC4 (GeneTex), eIF4A3, p53 (ProteinTech), Magoh, DNA-PK, Rad51 (Abcam), histone 3, Ku70, Ku80, ATR, phospho-Chk1 and phospho-Chk2 (Cell Signaling Technology).

Immunofluorescence
Immunofluorescence was performed essentially as described (Chuang et al., 2013). Polyclonal primary antibodies used were against Y14 (Bethyl), eIF4A3 (ProteinTech), CC3 (Cell Signaling) and 53BP1 (Novus), and monoclonal antibodies were against γH2AX (Millipore) and Y14 (Abcam). Secondary antibodies were conjugated with FITC or rhodamine (anti-mouse or anti-rabbit IgG, Cappel). Nuclei were counterstained with Hoechst 33258 or DAPI. The specimens were observed using a laser-scanning confocal microscope (LSM 780, Carl Zeiss) coupled with an image analysis system. To detect R-loops, cells were fixed in ice-cold methanol for 20 min, followed by hybridization overnight with antibody S9.6 (ENH001, Kerafast) and subsequently with FITC-conjugated anti-mouse IgG for 2 h. Visualization was performed using a laser-scanning microscope (LSM 700, Carl Zeiss).

Laser Microirradiation and Live-cell Imaging
The cDNAs encoding Ku70 and Ku80 were fused with the EGFP cDNA, cloned into a retrovirus vector pLNCX (Clontech), and used to transduce U2OS cells as described (Pan et al., 2015). U2OS cells stably expressing GFP-fused MDC1 were from a previous study (Chang et al., 2015). Cells were mounted onto the incubation stage in a SP5 X inverted confocal microscope (Leica Microsystems) supplemented with humidified 5% CO_2 at 37 °C. Laser-microirradiation was carried out using a laser diode (405 nm) with full output settings. Ten scans were applied to generate DNA damages restricted to the laser path with minimal cellular toxicity. Live-cell images were taken every 15 s using the same confocal microscope with the minimum-detectable output of a laser diode (488 nm). Fluorescence intensity was measured with ImageJ (National Institutes of Health, USA).

***In Vitro* Pull-down Assay**
Recombinant GST-Y14 fusion proteins (full-length, ΔN lacking the N-terminal 55 amino acids and ΔC lacking the C terminal 23 amino acids) have been previously described (Hsu Ia et al., 2005; Chuang et al., 2013). Phosphorylated Y14 was obtained by co-expression of SR protein kinase 1 and GST-Y14 in bacteria (Hsu Ia et al., 2005). For the *in vitro* pull down assay (Hsu Ia et al., 2005), 5 μg of GST or GST-Y14 (full-length, truncated or phosphorylated forms) was incubated with 50 μg of HeLa cell lysates. After extensive wash, bound proteins were analyzed by immunoblotting.

End-joining Assay

The procedure for the end-joining assay was as described (Seluanov et al., 2004). In brief, the NHEJ reporter was digested with *Hind*III or I-*Sce*I. U2OS cells were co-transfected with uncut or linearized reporter and an siRNA. For the rescue experiment, the expression vector for siY14-resistant FLAG-Y14 was used for co-transfected. The number of GFP-positive cells was determined 48 h post-transfection by fluorescence-activated cell sorting using 17-color LSR II Analytic Flow Cytometer (BD Biosciences).

Immunostaining of Embryonic Brain

Immunostaining of E13.5 mouse embryonic cortex was essentially described in (Silver et al., 2010). In brief, brain slices were fixed overnight in 4% paraformaldehyde at 4°C, followed by submersion in 30% sucrose. Brain cryostat sections were permeabilized with 0.2% Triton X-100 for 10 min, blocked with MOM block reagent (Vector Laboratories) for 1 h at room temperature, and incubated with appropriate antibodies (indicated in the text) overnight at 4°C. Finally, sections were incubated with an appropriate secondary antibody and stained with Hoechst 33258 (Sigma).

Dot Blot R-loop Assay

Genomic DNA was extracted from cells and subsequently treated (or not treated) with 50 U/ml RNase H (New England Biolabs). For assay, 100 ng of DNA was spotted onto a nitrocellulose membrane. The membrane was incubated with antibody S9.6 overnight, followed by incubation for 1 h with horseradish peroxidase-conjugated goat anti-mouse IgG (Santa Cruz Biotechnology). Signals were detected using the SuperSignal West Pico Chemiluminescent substrate (Thermo Fisher Scientific), and images were acquired using FlourChemQ (Protein Simple).

Immunoprecipitation of DNA-RNA Hybrids

DRIP was performed essentially according to Halasz et al. (Halasz et al., 2017). For each transfection, 6 µg of sonicated genomic DNA was incubated with 3-µg S9.6-conjugated protein A beads (10 µl) in the immunoprecipitation buffer (50 mM HEPES pH 7.5, 140 mM NaCl, 5 mM EDTA, 1% Triton X-100 and 0.1 % deoxycholate) at 4°C for 3 h. For RNase H treatment, the beads were incubated with 50 U RNase H (New England Biolabs) at 37˚C for 2.5 h; 10 mM EDTA was added to stop the reaction. Beads were washed extensively with the immunoprecipitation buffer and twice with 10 mM Tris-HCl (pH 8). DNA-RNA hybrids were eluted with a buffer containing 100 mM $NaHCO_3$ and 1% SDS for 10 min at 37˚C followed by phenol-chloroform extraction. qPCR was performed using specific primers (Table S2) with LightCycler 480 SYBR Green I Master (Roche) and analyzed with a QuantStudio 12K Flex Real-Time PCR System (Thermo Fisher Scientific).

Phosphate-Affinity Gel Electrophoresis

HEK293 cells were transfected with the vector encoding FLAG-Y14 or its non-phosphorylatable mutant. Cell lysate was fractionated on Phos-tag™ Acrylamide gel according to manufacturer’s instruction (Wako).

Statistical Analysis

Statistical analysis was performed using GraphPad Prism 7.0.

Supplemental References

Bhatia, V., Barroso, S.I., Garcia-Rubio, M.L., Tumini, E., Herrera-Moyano, E., and Aguilera, A. (2014). BRCA2 prevents R-loop accumulation and associates with TREX-2 mRNA export factor PCID2. Nature *511*, 362-365.

Britton, S., Coates, J., and Jackson, S.P. (2013). A new method for high-resolution imaging of Ku foci to decipher mechanisms of DNA double-strand break repair. J Cell Biol *202*, 579-595.

Chang, C.F., Chu, P.C., Wu, P.Y., Yu, M.Y., Lee, J.Y., Tsai, M.D., and Chang, M.S. (2015). PHRF1 promotes genome integrity by modulating non-homologous end-joining. Cell Death Dis *6*, e1716.

Chuang, T.W., Chang, W.L., Lee, K.M., and Tarn, W.Y. (2013). The RNA-binding protein Y14 inhibits mRNA decapping and modulates processing body formation. Mol Biol Cell *24*, 1-13.

Chuang, T.W., Peng, P.J., and Tarn, W.Y. (2011). The exon junction complex component Y14 modulates the activity of the methylosome in biogenesis of spliceosomal small nuclear ribonucleoproteins. J Biol Chem *286*, 8722-8728.

Gorski, J.A., Talley, T., Qiu, M., Puelles, L., Rubenstein, J.L., and Jones, K.R. (2002). Cortical excitatory neurons and glia, but not GABAergic neurons, are produced in the Emx1-expressing lineage. J Neurosci *22*, 6309-6314.

Gunn, A., Bennardo, N., Cheng, A., and Stark, J.M. (2011). Correct end use during end joining of multiple chromosomal double strand breaks is influenced by repair protein RAD50, DNA-dependent protein kinase DNA-PKcs, and transcription context. J Biol Chem *286*, 42470-42482.

Halasz, L., Karanyi, Z., Boros-Olah, B., Kuik-Rozsa, T., Sipos, E., Nagy, E., Mosolygo, L.A., Mazlo, A., Rajnavolgyi, E., Halmos, G., *et al.* (2017). RNA-DNA hybrid (R-loop) immunoprecipitation mapping: an analytical workflow to evaluate inherent biases. Genome Res *27*, 1063-1073.

Hsu Ia, W., Hsu, M., Li, C., Chuang, T.W., Lin, R.I., and Tarn, W.Y. (2005). Phosphorylation of Y14 modulates its interaction with proteins involved in mRNA metabolism and influences its methylation. J Biol Chem *280*, 34507-34512.

Lai, M.C., Chang, W.C., Shieh, S.Y., and Tarn, W.Y. (2010). DDX3 regulates cell growth through translational control of cyclin E1. Mol Cell Biol *30*, 5444-5453.

Lee, K.M., and Tarn, W.Y. (2014). TRAP150 activates splicing in composite terminal exons. Nucleic Acids Res *42*, 12822-12832.

Lu, C.C., Lee, C.C., Tseng, C.T., and Tarn, W.Y. (2017). Y14 governs p53 expression and modulates DNA damage sensitivity. Sci Rep *7*, 45558.

Mao, H., Pilaz, L.J., McMahon, J.J., Golzio, C., Wu, D., Shi, L., Katsanis, N., and Silver, D.L. (2015). Rbm8a haploinsufficiency disrupts embryonic cortical development resulting in microcephaly. J Neurosci *35*, 7003-7018.

Nowsheen, S., Xia, F., and Yang, E.S. (2012). Assaying DNA damage in hippocampal neurons using the comet assay. J Vis Exp, e50049.

Pan, W.A., Tsai, H.Y., Wang, S.C., Hsiao, M., Wu, P.Y., and Tsai, M.D. (2015). The RNA recognition motif of NIFK is required for rRNA maturation during cell cycle progression. RNA Biol *12*, 255-267.

Seluanov, A., Mittelman, D., Pereira-Smith, O.M., Wilson, J.H., and Gorbunova, V. (2004). DNA end joining becomes less efficient and more error-prone during cellular senescence. Proc Natl Acad Sci U S A *101*, 7624-7629.
Silver, D.L., Watkins-Chow, D.E., Schreck, K.C., Pierfelice, T.J., Larson, D.M., Burnetti, A.J., Liaw, H.J., Myung, K., Walsh, C.A., Gaiano, N., *et al.* (2010). The exon junction complex component Magoh controls brain size by regulating neural stem cell division. Nat Neurosci *13*, 551-558.